Fine-scale interplay between decline and growth determines the spatial recovery of coral communities within a reef

Abstract

As coral reefs endure increasing levels of disturbance, understanding patterns of recovery following disturbance(s) is paramount to assessing the sustainability of these ecosystems. Given the slow dynamics of coral reefs and the increasing frequency of environmental pressures, management strategies focus on understanding recovery patterns to drive efforts and actively promote the recovery of key coral populations. However, the fine spatial scale heterogeneity of coral dynamics challenges our capacity to understand recovery patterns at large spatial scales and guide effective management actions. In this study, we developed a spatio-temporal statistical model to estimate the long-term trajectories of branching, plate and massive corals at fine-spatial scales and predict their recovery pat-

terns at unobserved locations within a reef. We parameterized the model using repeated and georeferenced observations from 783 locations during 16 years at Heron Reef (Great Barrier Reef, Australia). We then developed indicators of recovery that capture the interplay between coral growth and relative decline from disturbance(s) across time, space and growth morphology. Our results reveal that successful recoveries, expressed in terms of probability, are associated with minimum growth rate thresholds of 4.3% and 6.4% (absolute growth, y^{-2}) for branching and plate corals in reef locations that were impacted by disturbance(s) at medium-high levels and historically abundant. As a product of the data revolution, predictive maps from statistical models support the development of new indicators that can support the identification of areas of concern to prioritise management intervention. They should be integrated into reef management toolbox along with other approaches.

Introduction

Impaired recovery of hard coral communities has mainly been attributed to cumulative disturbances (Halpern et al., 2008; Darling et al., 2013; Osborne et al., 2017; Vercelloni et al., 2017; Hughes et al., 2018; Ortiz et al., 2018; Mellin et al., 2019; Vercelloni et al., 2020; Bozec et al., 2022). The poor recovery of critical communities, including branching and plate coral morphologies, diminish their function as habitat providers and threatens the high marine diversity

associated with these species (Adjeroud et al., 2009; Fisher et al., 2015; Kayal et al., 2018; Ortiz et al., 2018; Darling et al., 2019). Traditionally, management strategies have focused on preserving ecosystem resilience (i.e., resistance and recovery) by reducing chronic pressures, such as nutrient pollution, overfishing, and predators, to enhance coral survival (Gilmour et al., 2013; Mcleod et al., 2019). More recently, active management interventions such as restoration are being explored to mitigate future effects of climate change by promoting faster rates of recovery, controlling chronic pressures and promoting the adaptive capacity of corals to thermal stress (Anthony et al., 2017). Notwithstanding these efforts, the effectiveness of management interventions is challenged by the impacts of large-scale climate-driven disturbances that spatially isolate disturbed from undisturbed reefs across hundreds of kilometres (Dietzel et al., 2021), inhibit connectivity and coral recruitment (Hughes et al., 2019) and may accentuate delays in coral reef recovery (Ortiz et al., 2018; Warne et al., 2022). Rapid assessment of the effectiveness of management interventions is one of the core challenges that need to be tackled to adapt management strategies in the light of new environmental regimes, and complex spatial dynamics (Anthony et al., 2020; Condie et al., 2021).

Modern coral reef management approaches propose using advanced technologies and analytical tools to model coral community coverage across space and time,

considering future changes in environmental conditions (Hickey et al., 2020). The final products include predictive maps of reef indicators across management areas. On the Great Barrier Reef (GBR), predictive maps have been developed based on diverse information, including drivers of coral dynamics, environmental gradients, exposure to disturbances from present and future regimes, greenhouse gas emissions and data integration from different monitoring programs, including citizen science and remote sensing (Mumby et al., 2014; De'ath et al., 2012; Wolff et al., 2018; Mellin et al., 2019; Peterson et al., 2020; Roelfsema et al., 2021; Bozec et al., 2022). A limitation of these maps is the dependence on coral reef monitoring data to predict changes at unobserved locations (Bozec et al., 2022). Uncertainty in predictions arises when monitoring observations are (1) too scarce in space to allow inferences about new locations, (2) not sufficiently representative across the combination of reef habitats and (3) too narrow with respect to types and exposures of disturbances and environmental gradients. This is particularly relevant to coral reef ecosystems when considering the high spatial heterogeneity of community composition resulting from complex space-time interactions throughout the time (Cumming et al., 2017). Consequently, robust estimation of coral cover trends at management scales (i.e., much larger than monitoring locations) continues to be a challenge (Vercelloni et al., 2017; Mellin et al., 2019). This motivates the development of spatially-explicit frame-

works that can better accommodate the fine spatial scale variability of community assemblages, recovery rates and susceptibility to a disturbance and provide management-ready products to inform effective decision-making.

Spatial patterns of coral reef recovery are driven by many variables acting at different spatial scales, including aspects of recent and past disturbance(s) (Connell et al., 1997; Graham et al., 2011; Ortiz et al., 2018; Mellin et al., 2019), community structure and demographic processes (Gilmour et al., 2013; Adjeroud et al., 2017; Kayal et al., 2018; Holbrook et al., 2018; Darling et al., 2019), and the environmental climatology of the habitats (Connell et al., 1997; Gouezo et al., 2019; Castro-Sanguino et al., 2021; Tebbett et al., 2022). Combined, this knowledge enables more accurate prediction of recovery dynamics of different populations and communities within a reef. Importantly, it provides more targeted information to manage recovery progress towards pre-disturbed states and associated demographic drivers (Kayal et al., 2018; Mellin et al., 2019; Darling et al., 2019).

However, these spatial patterns are typically estimated at discrete hierarchical spatial scales, including sites, reefs, habitats and regions to accommodate a high variability of recovery patterns within a reef (Hughes et al., 2012; Tebbett et al., 2022). The systematic lack of studies accounting for fine-scale variability highlights the need to explore the influence of space in the estimations of coral reef

recovery patterns to support model-based decision-support that better aligns with management goals (Zurell et al., 2022). By representing the space using continuous spatial processes, we allow information sharing between nearby locations and introduce a dependence (defined as spatial auto-correlation) into the observed data. Considering spatial dependency is key to estimating the spatial scale of coral recovery patterns and understanding the importance of drivers acting fine-scale, such as coral larval supply, coral recruitment and herbivory in shaping those patterns (Fletcher and Fortin, 2018).

Here, we developed a spatio-temporal model to (1) estimate long-term trajectories of three groups of hard corals based on their growth morphology, (2) extract the spatial auto-correlation from the data, (3) use these information to predict coral cover at unobserved locations within a reef and (4) develop new indicators of coral recovery. Since 2002, benthic communities have been monitored annually at Heron Reef, situated in the Southern Great Barrier Reef (Roelfsema et al., 2021). These surveys have captured 11 years of coral recovery (2008-2018) following the impacts of the white syndrome coral disease outbreak and storm damage. Spatial patterns are estimated using the complete time series (16 years, 2002-2018) of fine-scale observational changes in branching, plate and massive corals across different habitats. The new indicators capture important aspects of coral recovery that can be used to assess the potential success of restoration

measures and explore alternative management options in the light of new environmental regimes.

Methods

Heron Reef Benthic Surveys and Geomorphic Zonation

The Heron Island field survey was originally designed to develop annual benthic habitat maps of coral reef by integrating field data and satellite imagery (Roelfsema and Phinn, 2010). The benthic compositions are semi-automatically derived from georeferenced photoquadrat collected at 2-3m interval along a transect in different zones. Each photoquadrat represents a 1x1 m^2 footprint of the benthos (see Roelfsema et al. (2021) for additional details on the methodology). The geomorphic zones define different habitats across a reef that are formed by physical attributes including depth and wave exposure (Kennedy et al., 2020; Roelfsema et al., 2021). Using this method, Heron Reef is divided into four geomorphic zones (Figure 1a). The northern and southern reef slope areas are characterized by high and low wave intensities, respectively, and depth of 4-7m. The inner and outer reef flats are shallower areas (0-2m) without influences of wave exposure.

The composition of coral community is estimated using a convolutional neu-

ral network and point-sampling methodology (González-Rivero et al., 2020; Roelfsema et al., 2021). Coral communities are subsequently aggregated into branching, plate and massive coral types to produce relative abundances of each of the three types for each photoquadrat. Sub-sites are defined as areas of 100 m^2 in size in each surveyed year and generated using hierarchical clustering based on Euclidean distance between geo-located photoquadrats (Roelfsema et al., 2021). This method of data aggregation has been used previously to forecast the effects of multiple and intensifying disturbances in the northern GBR (Vercelloni et al., 2020), the efficiency of management zoning in Indonesia (Kennedy et al., 2020) and the identification of hotspots of coral cover across Heron Reef using the same datasets (Roelfsema et al., 2021).

The generated result is a total of 783 sub-sites based on an average of 8.7 ($\pm$ 4.6 standard deviation) photoquadrats per sub-site for each of the 16 years (2002-2018). The abundances of branching, plate and massive corals are then averaged within each sub-site and year. Observations of coral cover at the sub-site scale were used to model 16 years of coral changes across the habitats and three forms of corals within Heron Reef.

Spatio-temporal model for coral cover

Recently published studies have shown the importance of the spatial structure of benthic data to estimate long-term trajectories and highlight the strength of spatial clustering of coral communities (Aston et al., 2019; Ford et al., 2021; Levy et al., 2018). The typical methods employed in these papers characterize spatial auto-correlation across different forms of corals and reef locations and gain knowledge about the spatial scales on which ecological drivers are acting. We developed a spatio-temporal model to go beyond these approaches, with the goal of reusing the estimated spatial structure to interpolate coral cover at unobserved locations and thus increase the volume of information to interpret. This aim is the essence of modern spatial statistical modelling: to estimate spatial patterns while considering the effects of drivers in species responses, and interpolate over a continuous spatial field to predict responses at unobserved locations (Lindgren et al., 2011).

A spatio-temporal Bayesian model is developed to estimate the trajectories of three groups of corals from 2002 to 2018 (Eqs. 1). The cover of branching, plate and massive corals (y_{it}), for observations i sampled at location s_i and time t was modelled independently. For each model, a Beta distribution is used because observed values of coral cover are proportions bounded between 0 and 1. The Beta likelihood is parameterized in terms of a variance ϕ and linked to the linear

model components via a logit transformation (Ferrari and Cribari-Neto, 2004).

$$
\begin{aligned}
y_{it} &\sim \mathsf{Beta}\left(\phi, \text{logit}^{-1}(x_i^T \beta_j + r(s_i,t) + V_i)\right) \\
r(s_i,t) &= \omega \cdot r(s_i,t-1) + Z(s_i,t), \\
Z(s,t) &\overset{\text{ind}}{\sim} \mathscr{GP}(0,K), \quad t = 2002,\ldots,2018
\end{aligned}
\tag{1}
$$

where, $x_i^T \beta_j$ is a function of an intercept β_0 and the four habitats β_j and V_i independent random effects at the sub-site level. The spatio-temporal random effects, $r(s_i,t)$, is composed of a first-order autoregressive process, $\omega \cdot r(s_i,t-1)$, in time and a Gaussian field, $Z(s,t)$, that is approximated using a Gaussian Markov random field (GMRF) and a covariance kernel. The GMRF is approximated using a stochastic partial differential equation (Lindgren and Rue, 2015). See Appendix S1 for more information about the spatio-temporal modelling.

Indicators of coral recovery

The years of recovery were set from 2008 to 2018 because no coral loss attributable to documented disturbances that was reported during this period. Coral recovery followed the impacts of four years of white syndrome disease outbreak between

2004-2008 and storm damage in 2008 (Haapkylä et al., 2010; Roff et al., 2011). Despite the proximity of cyclone Hamish in 2009, there was no recorded impact on Heron Reef (Haapkylä et al., 2010).

Preliminary analyses presented in Appendix S2 showed that the use of partial recovery (80% of pre-disturbance values) instead of the full recovery (100% of pre-disturbance values) allowed almost double the number of reef locations to be considered as recovered. This is mostly due to the high pre-disturbance cover of branching corals in some locations of Heron Reef.

Probability of recovery

The probability of recovery was used to determine the outcome of recovery while considering uncertainty in the capability of branching and plate corals to recover from the disturbance(s). For every unobserved location $\hat{s}_i$, and coral morphology, the probability of recovery is estimated from the difference between predicted coral cover at time t of recovery (2008-2018) and their pre-disturbance values ($\widehat{y}_{\text{baseline}}$, Eq. 2).

$$\hat{p}_{\text{rec},t} = \frac{1}{2000}\sum_{k=1}^{2000} I\left\{\left(\widehat{y}_t^{(k)} - 0.8\widehat{y}_{\text{baseline}}^{(k)}\right) > 0\right\}, \quad t = 2008,\ldots,2018$$

$$\widehat{y}_{\text{baseline}} = \max_{t_{\text{baseline}} \in \{2002,\ldots,2007\}} \widehat{y}_{t_{\text{baseline}}} \qquad (2)$$

with 2000 corresponding to the number of draws from posterior distributions of estimated coral cover $\widehat{y}_{\hat{s}_i t}$.

Recovery was asserted when $\hat{p}_{\text{rec}}$ was greater than 0.75 at any time during the years of recovery and locations $\hat{s}_i$. When this condition was satisfied, recovery was defined as successful. As such, successful recovery is interpreted as "75% chance of recovering to at least 80% of pre-2008 coral cover".

Growth rate

The growth rate corresponds to the absolute growth rate between two consecutive sampling periods because hard corals are growing slowly. It is estimated from the posterior distributions of the differences between $\widehat{y}_t^{(k)}$ and $\widehat{y}_{t-2}^{(k)}$ for every k draws (Eq. 3).

$$\mathsf{GrowthRate}(t) = \frac{1}{2000}\sum_{k=1}^{2000}\left(\widehat{y}_t^{(k)} - \widehat{y}_{t-2}^{(k)}\right), \quad t = 2010,\ldots,2018 \qquad (3)$$

A total of 2000 draws from the predictive posterior distributions were used to estimate the growth rate. The average growth rate and associated 95% credible intervals are estimated using the percentiles (50%, 2.5% and 97.5% respectively).

Relative decline

The relative decline expressed the amount of coral loss from disturbance(s). It was estimated using the maximum predicted coral cover pre-disturbance, $\widehat{y}_{\text{baseline}}$, at every predictive location and its corresponding value in 2008 (Eq. 4).

$$\mathsf{RelativeDecline} = \frac{\widehat{y}_{2008} - \widehat{y}_{\text{baseline}}}{\widehat{y}_{\text{baseline}}} \tag{4}$$

The average decline and associated 95% credible intervals were then categorized into levels of decline (low, medium, high) using the percentiles (50%, 2.5% and 97.5% respectively).

Growth rate thresholds

Absolute growth rates and probability of recovery were used to estimate minimum growth rate thresholds that ensured recovery. To do this, we developed

logistic models for branching and plate corals with probability of recovery as response variables transformed into binary data with 1 when $\hat{p}_{\text{rec}}$ were greater than 75% chance of recovery and 0 otherwise. Logistic models were fit on the reef slope south locations for the branching corals in 2014 and reef slope north locations for the plate in 2016. We assumed that these years matched with the beginning of the exponential phase of coral growth as described in (Ortiz et al., 2018). The thresholds were defined when the probabilities of recovery (i.e >75% chance of recovering to at least 80% of pre-2008 coral cover) estimated by the logistic models were greater than 50%.

Implementation

Spatio-temporal Bayesian model

Model outputs were used to predict values of coral cover across the entire Heron Reef. To do this, the reef was divided into 2,384 locations (Figure 1b) and predictive values and associated uncertainties were estimated for each of these new locations and surveyed years. The presence of residual spatial and temporal auto-correlation was tested using the DHARMa (Hartig, 2019) and glmmTMB (Brooks et al., 2017) R packages. The spatio-temporal model was implemented using the r-INLA package (Rue et al., 2017) and run on a high-performance computer. The best model formulations were retained using visual and statis-

tical diagnostics including model fit, residual patterns, basis dimensions, distributional assumption, and Akaike Information Criterion values (AIC). Autocorrelation tests, computational details of fitting the models, as well as prior specifications, are provided in Appendix S1.

Indicators of recovery

Indicators were estimated at 2384 predictive locations s_i across Heron Reef but interpreted within a smaller area on the western side of the reef (Figure 1b). This area corresponded to the geographical extent of the data and included 481 locations. This step ensured the detection of signals from the indicators of recovery due to a higher uncertainty associated with the spatial predictions at locations further away from the data (see Appendix S1). Indicators were also estimated at the habitat scale by averaging the values within the same habitat and associated uncertainty for a given year. The logistic models were developed using the R package "brms" (Bürkner, 2017) and thresholds were estimated by averaging model outputs from 100 model iterations (see Appendix S1).

Results and Discussion

Temporal changes of coral communities

Pre-disturbance (2002-2008)

In the period 2002-2008, before the major environmental disturbance(s), branching corals were abundant in the southern and northern slopes of Heron Reef (Figure 2a). The maximum coverage is estimated at 37.3% (27.6-47.4%, 95% CI) in 2004 and 24.9% (17.1-33.8%) in 2006, respectively. A sizeable relative decline of branching corals is estimated in these habitats, with 93.4% loss (86.8-97.3%) in four years for the south slope and 83.5% loss (71.8-91.9%) in five years for the northern slope.

Plate corals dominated the northern slopes (Figure 2b) with maximum coverage of 26.4 % (19.4-34.0%) in 2004, decreasing to a minimum of 7.7% (5.0-11%) in 2010 (70.8 % 58.3-72.7%, relative decline). Studies by (Haapkylä et al., 2010) and (Roff et al., 2011) described the extirpation of corals, including plate corals during the major disease outbreak in 2004-2008 at different sites within these habitats with a shift in coral composition from plate to bushy corals.

Post-disturbance (2008-2018)

Branching corals mostly grew in the sheltered areas of the Reef Slope South (Figure 2a) that are protected from high wave exposure by adjacent reefs, including Wistari, Sykes, and One Tree Reefs (Connell et al., 1997). In this habitat, the model estimates a relative increase of 1527 % (720-1587%) from 2008 to 2014, with a maximum amount of cover of 40.2 % (31.9-48.7%). Branching in the northern slope increased to a maximum of 13.8% (9.0-19.3%) in this period. Plate corals grew in the southern and northern slopes of Heron Reef to reach maximum values that were higher than pre-disturbance values (Figure 2b). The prominent increase for plate corals occurred on the Reef Slope North, which is more exposed to frequent and higher intensity waves than the southern reef slope. In the northern slope, plate corals increased to 27.1% (20.9-33.7%) in 2018 and 18.1% (13.3-23.5%) in 2016 for the south habitat.

Through the years of recovery, coral community composition changed with a net dominance of plate corals in the northern section of the reef. The lack of recovery for branching corals cannot be explained by the nature of the disturbance as there is no clear evidence of what had impacted this reef section (Haapkylä et al., 2010; Roff et al., 2011). Differences in wave exposure between north and south and the high prevalence of branching corals in the southern reef slope before the decline may have contributed to the rapid southern recovery due to their strong

capability of recovery after fragmentation (Lirman, 2000). The study from (Connell et al., 1997) indicated differences between mechanisms of declines and recoveries in northern and southern sections of Heron Island. Our model estimates suggest that plate corals were able to recover from disease outbreaks, but this is less evident for branching corals on the northern slope. Coral colony size is an important factor associated with this type of disturbance (Roff et al., 2011), but the size was not recorded as part of the Heron survey.

Spatial indicators of coral recovery

Probability of recovery and associated growth rate

Coral recovery is defined when a reef location reached 80% of its pre-disturbance value with the pre-disturbance value corresponding to the maximum estimated cover before 2008. As expected, branching corals were abundant in the southern slope from 2002 to 2005, then decreased until 2008 and recovered gradually until 2018 (Figure 3a). The rapid recovery is reflected by the dynamics of the probability of recovery showing less than 75% chance of recovery from 2008 (36.6%, 12.4 - 64.0%) to 2012 (62.6%, 13.9 - 86.7%) and then high probabilities of recovery (greater than the threshold of 0.75) from this year (Figure 3b). In these locations, the growth rate increased from 4.8% (2.2 - 6.8 % y^{-2} between 2010-2012 to a maximum of 10.4% (7.5 - 13.3 % y^{-2}) until 2014 (Figure 3c).

Thereafter, the growth decreased to negative values reaching 4.5 % (6.8 - 2.4% y^{-2}) in 2018. This decline in branching growth is likely related to a reduction in space availability during the years of recovery. The probability of recovery remained low for the northern slope habitat (Figure 3b), associated with a negative growth rate at the beginning and end of the surveyed years (-4.4%, -6.1 - -2.9% y^{-2} in 2008 and -1.3%, -2.9 - -0.1% y^{-2} in 2018) and a positive growth rate ranging between 1-2% between these years (Figure 3c).

Plate corals recovered in the slope habitat in the north and south during the surveyed period (Figure 4a). On the south slope, the probability of recovery was estimated at 98.3% (86.8 - 99.8%) in 2008 and remained above this value until 2018, despite a low growth rate of 3.0% (1.2 - 7.8%) estimated in 2014 (Figure 4b). On the north slope, the probability of recovery was almost zero for the first four years of the recovery phase and increased rapidly between 2012 and 2014 to reach more than 75% chance of recovery in 2014-2018 (Figure 4b). In these locations, the growth rate increased from - 1.3% y^{-2} (-2.2 - -0.1% y^{-2}) in 2008 to 12.2% y^{-2} (8.7 - 15.8% y^{-2}) in 2014 before being negative again (-0.2% y^{-2}, -2.0 - 0.9% y^{-2}) in 2016 (Figure 4c). This rapid increase is the signature of plate corals that use the first years of recovery to build the base of their colony and then expand exponentially due to high growth rates and potential large sizes associated with their growth morphology (Ortiz et al., 2021).

Growth rate, relative decline and cover baseline

Overall, branching corals recovered (to within 80% of baseline) at 53.4% of locations across the north and south reef slopes in 6.90 years ($\pm$ 1.25 SD). The fastest recovery occurred in six years at 20 locations within the south slope, and the longest recovery was estimated at ten years at three locations on the north slope. Most of the reef locations recovered on the south slope (87.1%)m compared with 12.9% of locations on the north slope (Figure 5a). On the south slope, locations that recovered were medium (15-37% relative decline) to highly ($>$ 37% relative decline) impacted by the disturbance(s) (Figure 5b). The cover baseline was mostly high ($>$ 40% branching cover) and medium (20-40% branching cover, Figure 5c). Branching corals at most of the locations grew above the growth rate threshold estimated at 4.30% y^{-2} ($\pm$ 0.01 SD) from the logistic model in 2012 and 2014 (Figure 5d, Appendix S2). Only four years of high growth rate were needed to recover branching corals in previously abundant places and medium-highly impacted by disturbance(s). The disturbances highly impacted branching corals in the north slope (Figure 5b). The low baseline abundance of branching corals in these locations (Figure 5c) is likely related to the low growth rate (Figure 5d) due to environmental conditions that are not favourable for this form of corals (Connell et al., 1997; Tanner, 2017). The high decline in branching ($>$ 37% relative decline) in association with a low growth rate re-

sulted in a lack of recovery for most of the locations in the north slope. However, the medium-high relative decline did not interfere with the recovery of branching corals in the southern slope because environmental conditions are prone to a fast growth rate, as shown by the medium-high cover baseline.

The recovery of plate corals was more generally spread across the north and south slopes, with 91.4% of locations showing recovery in 6.87 years ($\pm$ 2.43 SD). The fastest recovery occurred in only two years at eight locations in the south slope but it took a maximum of ten years to recover for six locations. More locations recovered in the south slope (58.5%) compared to the north slope (41.5%, Figure 6a). The highest decline occurred in the north slope with some loss estimated at more than 58% (Figure 6b) in locations with medium (13-27%) and high ($>$ 27%) cover baseline (Figure 6c). Plate corals at locations the most impacted by the disturbance(s) grew the fastest with a maximum growth rate estimated around 20% y^{-2} in 2016 and above the growth rate threshold of 6.31% y^{-2} ($\pm$ 0.02 SD) in 2014 (Figure 6d, Appendix S2). Plate corals at locations that were impacted by disturbance(s) at a medium level grew above this threshold in 2016, and locations impacted at a low level never reached the threshold. These results emphasize the interplay between relative decline and growth rate by creating free space for new plate recruits to settle after the disturbance(s) in 2008 and grow until saturation in 2018. In a paper dedicated to tabular *Acropora*,

Ortiz et al. (2021) describes the complex mechanism of coral settlement that is enhanced by the presence of dead colonies. Plate corals were mostly impacted by coral diseases that are known to preserve the dead skeletons of the corals on which algae and potential new recruits can settle. They also show high potential connectivity from locations that were less impacted by the disturbance(s) and favourable environmental conditions suggested by the high and medium levels in the cover baseline before the disturbance(s). The last point has also been relevant for the branching corals, where the recovery occurred in locations that were historically abundant.

Spatial auto-correlation during coral recovery

The presence of spatial and temporal auto-correlation in the long-term data of Heron Reef has been demonstrated by (Connell et al., 1997). In this study, we refined this knowledge by quantifying spatial dependence during the recovery of different forms of corals after accounting for the habitat effect defined by geomorphic zones. Our findings show that the spatial auto-correlation is within the same range as that estimated by (Connell et al., 1997) (up to 800m) but that this varies by coral morphology. Spatial ranges were estimated as 1.02km (0.75 - 1.30km, 95% CI), 1.46km (1.07 - 1.90km) and 12.76km (7.24 - 18.97km) for branching, plate and massive corals, respectively (Appendix S1). The presence

of spatial auto-correlation is explained by the mechanisms of coral recruitment that are related to the supply of larvae from plankton, suitability of substrate for coral settlement and mortality post-settlement (Connell et al., 1997). Among these factors, only the supply of larvae from plankton has the potential to act at the kilometre scale in conjunction with the interaction between habitat and currents that drive the number of new recruits in these areas (Tebbett et al., 2022). Connell et al. (1997) and Tanner (2017) suggested that the supply of plankton is likely to be higher on the southern slope of Heron Reef due to the proximity to other reefs, which increases coral recovery rates. However, we found that branching corals drove the recovery on the south slope and plate corals on the north slope. Further investigations should focus on the interactions between branching and plate corals within habitats to better understand the influences of connectivity, demographic traits of coral forms and competition for space in driving recovery patterns.

Analytical approaches to improve the effectiveness of long-term monitoring and increase the amount of knowledge extracted from the data have been applied to coral reefs (Kang et al., 2016; Thilan et al., 2019; Mellin et al., 2020). The quantification of spatial auto-correlation is informative for the design of coral reef monitoring (Hamylton, 2013). Using a combination of spatio-temporal modelling and fine-scale data, the estimated values of spatial ranges reveal that

surveyed locations separated by 1km and 1.5km can be considered pseudo-replicated observations for branching and plate corals during recovery, respectively. The presence of redundant information in monitoring data violates the assumption of independence between observations in traditional statistical tests, which may bias ecological interpretations (Ver Hoef et al., 2018) about drivers of coral recovery. We recommend that future surveys that aim to understand mechanisms underlying coral recovery should ensure that the survey includes locations within and between a radius of 1.5km allowing for replications and collection of data that are not spatially auto-correlated. Locations should also be sampled across different habitats, especially in more than one flank of the reef slope. In this way, monitoring surveys can provide an optimized amount of ecological and spatial information about the recovery patterns of the entire coral community.

Spatio-temporal modelling for coral reef data

Analyses of the influence of spatial variation during years of recovery allowed us to identify spatial patterns of recovery for different types of corals within a reef. The application of spatio-temporal models to this unique dataset reveals that consideration of interactions between space and time is essential in order to predict recovery patterns and investigate the fine-scale variability of coral

dynamics (Appendix S1). Such interactions are challenging to compute, even using Bayesian approaches, but improvements in the field of computational science and applied statistics will ease their inclusion in future statistical modelling frameworks (Wikle and Zammit-Mangion, 2022). Moreover, these computational improvements will enable the scaling-up of the approach to more than one reef.

We acknowledge that the high volume of data needed in order to fully exploit the benefits of spatio-temporal statistical models is another limiting condition in the field of coral reef research. Additional work is needed to estimate the minimum amount of data that will enable the implementation of spatio-temporal models to more than one reef. The development of new coral-reef monitoring techniques, including the use of machine learning (González-Rivero et al., 2020), citizen science (Santos-Fernandez et al., 2021) and combined approaches (Peterson et al., 2020) to boost collection, processing and exploration of reef data and their democratization are rapidly being adopted by research and governmental institutions across the Indo-Pacific. In combination with advanced modelling techniques able to handle large and complex datasets, outputs from data-driven approaches should be systematically integrated into the reef management toolbox (Zurell et al., 2022). They are keys to providing rapid and up-to-date information to reef managers, supporting the development of adaptive strategies and assess-

ment of management interventions.

Conclusions

The spatial mismatch between the large spatial scale of climate-driven disturbances and the finer spatial scale of management interventions (Cumming et al., 2017; Bellwood et al., 2019) forces the development and implementation of new types of measures to support coral recovery (Anthony et al., 2020). In this study, we developed new indicators of coral recovery that have been estimated based on the fine spatial scale variability of coral changes within a reef and the spatio-temporal structures of data. The resulting predictive maps of indicators of coral recovery across Heron Reef show clear zonation of recovery probabilities that is different between coral morphology and related to the decline from disturbance(s) and historical abundance.

If management interventions ignore this information and only use locations where long-term monitoring sites are located, the benefits of interventions may be lost because of uninformed spatial prioritization (Anthony et al., 2020). This is especially important considering that existing monitoring only represents 40% of the environmental regimes of the GBR (Mellin et al., 2020). Importantly, because the scale for management of local stressors is only a fraction of the global scale of influence of climate change, managers are likely to be forced to increas-

ingly consider prioritization of reef areas with high intrinsic resilience capacity (GAME et al., 2008). Predictive maps from spatio-temporal models have the potential to fill a gap by gathering information from existing knowledge underlying coral recovery, learning from data to infer at unobserved locations and developing useful indicators for decision-making.

Data Science, including the combination of machine learning algorithms to rapidly process a large amount of information and statistical modelling to develop robust ecological knowledge, has the potential to radically change the way of managing coral reef. The use of this approach is still in its infancy in Australia, but current research efforts bridge the gap between data scientists, coral reef ecologists and reef managers to provide more comprehensive information about the decline of the condition of coral reef habitats in the Great Battier Reef and support the development of mitigation interventions under future climate scenarios. Importantly, while there is an increasing trend of incorporating climate change into spatial prioritisation, serious gaps still exist in current methodologies (Jones et al., 2016). This study provides a contribution to this increasingly challenging field by developing methodologies that recognise discrete and long-term impacts on ecosystem recovery potential. Our approach can be easily integrated into broader spatial prioritisation frameworks that respond to spatial and temporal scales of the processes being managed.

Data archiving statement

Data are already published and publicly available, with those items properly cited in this submission. Data sets utilized for this research are as follows: https://doi.pangaea.de/10.1594/PANGAEA.907025 (Roelfsema et al., 2019) and https://doi.org/10.6084/m9.figshare.14034320.v1 (Roelfsema et al., 2021).

References

Adjeroud, M., M. Kayal, and L. Penin (2017). Importance of recruitment processes in the dynamics and resilience of coral reef assemblages. *Marine animal forests 549*, 569.

Adjeroud, M., F. Michonneau, P. Edmunds, Y. Chancerelle, T. L. De Loma, L. Penin, L. Thibaut, J. Vidal-Dupiol, B. Salvat, and R. Galzin (2009). Recurrent disturbances, recovery trajectories, and resilience of coral assemblages on a south central pacific reef. *Coral Reefs 28*(3), 775–780.

Anthony, K., L. K. Bay, R. Costanza, J. Firn, J. Gunn, P. Harrison, A. Heyward, P. Lundgren, D. Mead, T. Moore, et al. (2017). New interventions are needed to save coral reefs. *Nature ecology & evolution 1*(10), 1420–1422.

Anthony, K. R., K. J. Helmstedt, L. K. Bay, P. Fidelman, K. E. Hussey, P. Lundgren, D. Mead, I. M. McLeod, P. J. Mumby, M. Newlands, et al. (2020). In-

terventions to help coral reefs under global change—a complex decision challenge. *Plos one 15*(8), e0236399.

Aston, E. A., G. J. Williams, J. M. Green, A. J. Davies, L. M. Wedding, J. M. Gove, J.-B. Jouffray, T. T. Jones, and J. Clark (2019). Scale-dependent spatial patterns in benthic communities around a tropical island seascape. *Ecography 42*(3), 578–590.

Bellwood, D. R., M. S. Pratchett, T. H. Morrison, G. G. Gurney, T. P. Hughes, J. G. Álvarez-Romero, J. C. Day, R. Grantham, A. Grech, A. S. Hoey, et al. (2019). Coral reef conservation in the anthropocene: Confronting spatial mismatches and prioritizing functions. *Biological conservation 236*, 604–615.

Bozec, Y.-M., K. Hock, R. A. Mason, M. E. Baird, C. Castro-Sanguino, S. A. Condie, M. Puotinen, A. Thompson, and P. J. Mumby (2022). Cumulative impacts across australia's great barrier reef: A mechanistic evaluation. *Ecological Monographs 92*(1), e01494.

Brooks, M. E., K. Kristensen, K. J. Van Benthem, A. Magnusson, C. W. Berg, A. Nielsen, H. J. Skaug, M. Machler, and B. M. Bolker (2017). glmmtmb balances speed and flexibility among packages for zero-inflated generalized linear mixed modeling. *The R journal 9*(2), 378–400.

Bürkner, P.-C. (2017). brms: An r package for bayesian multilevel models using stan. *Journal of statistical software 80*, 1–28.

Castro-Sanguino, C., J. C. Ortiz, A. Thompson, N. H. Wolff, R. Ferrari, B. Robson, M. M. Magno-Canto, M. Puotinen, K. E. Fabricius, and S. Uthicke (2021). Reef state and performance as indicators of cumulative impacts on coral reefs. *Ecological Indicators 123*, 107335.

Condie, S. A., K. R. Anthony, R. C. Babcock, M. E. Baird, R. Beeden, C. S. Fletcher, R. Gorton, D. Harrison, A. J. Hobday, É. E. Plagányi, et al. (2021). Large-scale interventions may delay decline of the great barrier reef. *Royal Society Open Science 8*(4), 201296.

Connell, J. H., T. P. Hughes, and C. C. Wallace (1997). A 30-year study of coral abundance, recruitment, and disturbance at several scales in space and time. *Ecological Monographs 67*(4), 461–488.

Cumming, G. S., T. H. Morrison, and T. P. Hughes (2017). New directions for understanding the spatial resilience of social–ecological systems. *Ecosystems 20*(4), 649–664.

Darling, E. S., T. R. McClanahan, and I. M. Côté (2013). Life histories predict coral community disassembly under multiple stressors. *Global Change Biology 19*(6), 1930–1940.

Darling, E. S., T. R. McClanahan, J. Maina, G. G. Gurney, N. A. Graham, F. Januchowski-Hartley, J. E. Cinner, C. Mora, C. C. Hicks, E. Maire, et al. (2019). Social–environmental drivers inform strategic management of coral reefs in the anthropocene. *Nature ecology & evolution 3*(9), 1341–1350.

De'ath, G., K. E. Fabricius, H. Sweatman, and M. Puotinen (2012). The 27–year decline of coral cover on the great barrier reef and its causes. *Proceedings of the National Academy of Sciences 109*(44), 17995–17999.

Dietzel, A., S. R. Connolly, T. P. Hughes, and M. Bode (2021). The spatial footprint and patchiness of large-scale disturbances on coral reefs. *Global Change Biology 27*(19), 4825–4838.

Ferrari, S. and F. Cribari-Neto (2004). Beta regression for modelling rates and proportions. *Journal of applied statistics 31*(7), 799–815.

Fisher, R., R. A. O'Leary, S. Low-Choy, K. Mengersen, N. Knowlton, R. E. Brainard, and M. J. Caley (2015). Species richness on coral reefs and the pursuit of convergent global estimates. *Current Biology 25*(4), 500–505.

Fletcher, R. and M. Fortin (2018). *Spatial ecology and conservation modeling*. Springer.

Ford, H. V., J. M. Gove, A. J. Davies, N. A. Graham, J. R. Healey, E. J. Conklin, and G. J. Williams (2021). Spatial scaling properties of coral reef benthic communities. *Ecography 44*(2), 188–198.

GAME, E. T., E. McDONALD-MADDEN, M. L. PUOTINEN, and H. P. POSSINGHAM (2008). Should we protect the strong or the weak? risk, resilience, and the selection of marine protected areas. *Conservation Biology 22*(6), 1619–1629.

569 Gilmour, J. P., L. D. Smith, A. J. Heyward, A. H. Baird, and M. S. Pratchett
570 (2013). Recovery of an isolated coral reef system following severe distur-
571 bance. *Science 340*(6128), 69–71.

572 González-Rivero, M., O. Beijbom, A. Rodriguez-Ramirez, D. E. Bryant,
573 A. Ganase, Y. Gonzalez-Marrero, A. Herrera-Reveles, E. V. Kennedy, C. J.
574 Kim, S. Lopez-Marcano, et al. (2020). Monitoring of coral reefs using ar-
575 tificial intelligence: A feasible and cost-effective approach. *Remote Sens-*
576 *ing 12*(3), 489.

577 Gouezo, M., Y. Golbuu, K. Fabricius, D. Olsudong, G. Mereb, V. Nestor,
578 E. Wolanski, P. Harrison, and C. Doropoulos (2019). Drivers of recovery
579 and reassembly of coral reef communities. *Proceedings of the Royal Society*
580 *B 286*(1897), 20182908.

581 Graham, N., K. Nash, and J. Kool (2011). Coral reef recovery dynamics in a
582 changing world. *Coral Reefs 30*(2), 283–294.

583 Haapkylä, J., J. Melbourne-Thomas, M. Flavell, and B. Willis (2010). Spa-
584 tiotemporal patterns of coral disease prevalence on heron island, great barrier
585 reef, australia. *Coral Reefs 29*(4), 1035–1045.

586 Halpern, B. S., K. L. McLeod, A. A. Rosenberg, and L. B. Crowder (2008).
587 Managing for cumulative impacts in ecosystem-based management through
588 ocean zoning. *Ocean & Coastal Management 51*(3), 203–211.

589 Hamylton, S. (2013). Five practical uses of spatial autocorrelation for studies of
590 coral reef ecology. *Marine Ecology Progress Series 478*, 15–25.

591 Hartig, F. (2019). Dharma: residual diagnostics for hierarchical (multi-
592 level/mixed) regression models. *R package version 0.2 4*.

593 Hickey, S. M., B. Radford, C. M. Roelfsema, K. E. Joyce, S. K. Wilson,
594 D. Marrable, K. Barker, M. Wyatt, H. N. Davies, J. X. Leon, J. Duncan, T. H.
595 Holmes, A. J. Kendrick, J. N. Callow, and K. Murray (2020). Between a reef
596 and a hard place: Capacity to map the next coral reef catastrophe. *Frontiers in*
597 *Marine Science 7*.

598 Holbrook, S. J., T. C. Adam, P. J. Edmunds, R. J. Schmitt, R. C. Carpenter, A. J.
599 Brooks, H. S. Lenihan, and C. J. Briggs (2018). Recruitment drives spatial
600 variation in recovery rates of resilient coral reefs. *Scientific reports 8*(1), 1–11.

601 Hughes, T. P., K. D. Anderson, S. R. Connolly, S. F. Heron, J. T. Kerry, J. M.
602 Lough, A. H. Baird, J. K. Baum, M. L. Berumen, T. C. Bridge, et al. (2018).
603 Spatial and temporal patterns of mass bleaching of corals in the anthropocene.
604 *Science 359*(6371), 80–83.

605 Hughes, T. P., A. H. Baird, E. A. Dinsdale, N. A. Moltschaniwskyj, M. S. Pratch-
606 ett, J. E. Tanner, and B. L. Willis (2012). Assembly rules of reef corals are
607 flexible along a steep climatic gradient. *Current Biology 22*(8), 736–741.

608 Hughes, T. P., J. T. Kerry, A. H. Baird, S. R. Connolly, T. J. Chase, A. Dietzel,
609 T. Hill, A. S. Hoey, M. O. Hoogenboom, M. Jacobson, et al. (2019). Global

warming impairs stock–recruitment dynamics of corals. *Nature 568*(7752), 387–390.

Jones, K. R., J. E. Watson, H. P. Possingham, and C. J. Klein (2016). Incorporating climate change into spatial conservation prioritisation: A review. *Biological Conservation 194*, 121–130.

Kang, S. Y., J. M. McGree, C. C. Drovandi, M. J. Caley, and K. L. Mengersen (2016). Bayesian adaptive design: improving the effectiveness of monitoring of the great barrier reef. *Ecological applications 26*(8), 2637–2648.

Kayal, M., H. S. Lenihan, A. J. Brooks, S. J. Holbrook, R. J. Schmitt, and B. E. Kendall (2018). Predicting coral community recovery using multi-species population dynamics models. *Ecology letters 21*(12), 1790–1799.

Kennedy, E. V., C. Roelfsema, M. Lyons, E. Kovacs, R. Borrego-Acevedo, M. Roe, S. Phinn, K. Larsen, N. Murray, D. Yuwono, et al. (2020). Reef cover: a coral reef classification for global habitat mapping from biophysical remote sensing. *bioRxiv*.

Kennedy, E. V., J. Vercelloni, B. P. Neal, D. E. Bryant, A. Ganase, P. Gartrell, K. Brown, C. J. Kim, M. Hudatwi, A. Hadi, et al. (2020). Coral reef community changes in karimunjawa national park, indonesia: Assessing the efficacy of management in the face of local and global stressors. *Journal of Marine Science and Engineering 8*(10), 760.

Levy, J., C. Hunter, T. Lukacazyk, and E. C. Franklin (2018). Assessing the spatial distribution of coral bleaching using small unmanned aerial systems. *Coral Reefs 37*(2), 373–387.

Lindgren, F. and H. Rue (2015). Bayesian spatial modelling with R-INLA. *Journal of Statistical Software 63*(19), 1–25.

Lindgren, F., H. Rue, and J. Lindström (2011). An explicit link between Gaussian fields and Gaussian Markov random fields: The stochastic partial differential equation approach. *Journal of the Royal Statistical Society: Series B (Statistical Methodology) 73*(4), 423–498.

Lirman, D. (2000). Fragmentation in the branching coral acropora palmata (lamarck): growth, survivorship, and reproduction of colonies and fragments. *Journal of Experimental Marine Biology and Ecology 251*(1), 41–57.

Mcleod, E., K. R. Anthony, P. J. Mumby, J. Maynard, R. Beeden, N. A. Graham, S. F. Heron, O. Hoegh-Guldberg, S. Jupiter, P. MacGowan, et al. (2019). The future of resilience-based management in coral reef ecosystems. *Journal of environmental management 233*, 291–301.

Mellin, C., S. Matthews, K. R. Anthony, S. C. Brown, M. J. Caley, K. A. Johns, K. Osborne, M. Puotinen, A. Thompson, N. H. Wolff, et al. (2019). Spatial resilience of the great barrier reef under cumulative disturbance impacts. *Global change biology 25*(7), 2431–2445.

Mellin, C., E. Peterson, M. Puotinen, and B. Schaffelke (2020). Representation and complementarity of the long-term coral monitoring on the great barrier reef. *Ecological Applications 30*(6), e02122.

Mellin, C., A. Thompson, M. J. Jonker, and M. J. Emslie (2019). Cross-shelf variation in coral community response to disturbance on the great barrier reef. *Diversity 11*(3), 38.

Mumby, P. J., N. H. Wolff, Y.-M. Bozec, I. Chollett, and P. Halloran (2014). Operationalizing the resilience of coral reefs in an era of climate change. *Conservation Letters 7*(3), 176–187.

Ortiz, J. C., R. J. Pears, R. Beeden, J. Dryden, N. H. Wolff, M. d. C. Gomez Cabrera, and P. J. Mumby (2021). Important ecosystem function, low redundancy and high vulnerability: The trifecta argument for protecting the great barrier reef's tabular acropora. *Conservation Letters 14*(5), e12817.

Ortiz, J.-C., N. H. Wolff, K. R. Anthony, M. Devlin, S. Lewis, and P. J. Mumby (2018). Impaired recovery of the great barrier reef under cumulative stress. *Science advances 4*(7), eaar6127.

Osborne, K., A. A. Thompson, A. J. Cheal, M. J. Emslie, K. A. Johns, M. J. Jonker, M. Logan, I. R. Miller, and H. P. Sweatman (2017). Delayed coral recovery in a warming ocean. *Global change biology 23*(9), 3869–3881.

Peterson, E. E., E. Santos-Fernández, C. Chen, S. Clifford, J. Vercelloni, A. Pearse, R. Brown, B. Christensen, A. James, K. Anthony, et al. (2020).

Monitoring through many eyes: Integrating disparate datasets to improve monitoring of the great barrier reef. *Environmental Modelling & Software 124*, 104557.

Roelfsema, C., E. M. Kovacs, K. Markey, J. Vercelloni, A. Rodriguez-Ramirez, S. Lopez-Marcano, M. Gonzalez-Rivero, O. Hoegh-Guldberg, and S. R. Phinn (2021). Benthic and coral reef community field data for heron reef, southern great barrier reef, australia, 2002–2018. *Scientific data 8*(1), 1–7.

Roelfsema, C., E. M. Kovacs, J. Vercelloni, K. Markey, A. Rodriguez-Ramirez, S. Lopez-Marcano, M. Gonzalez-Rivero, O. Hoegh-Guldberg, and S. R. Phinn (2021). Fine-scale time series surveys reveal new insights into spatio-temporal trends in coral cover (2002–2018), of a coral reef on the southern great barrier reef. *Coral Reefs*, 1–13.

Roelfsema, C. M., E. M. Kovacs, K. Markey, and S. R. Phinn (2019). Benthic and substrate cover data derived from field photo-transect surveys for the Heron Reef flat and slope areas (2002-11). PANGAEA. In: Roelfsema, Christiaan M; Kovacs, Eva M; Stetner, Douglas; Phinn, Stuart R (2018): Georeferenced benthic photoquadrats captured annually from 2002-2017, distributed over Heron Reef flat and slope areas. PANGAEA, https://doi.org/10.1594/PANGAEA.894801.

Roelfsema, C. M. and S. R. Phinn (2010). Integrating field data with high spatial resolution multispectral satellite imagery for calibration and validation of

coral reef benthic community maps. *Journal of Applied Remote Sensing 4*(1), 043527.

Roff, G., E. C. E. Kvennefors, M. Fine, J. Ortiz, J. E. Davy, and O. Hoegh-Guldberg (2011). The ecology of 'acroporid white syndrome', a coral disease from the southern great barrier reef. *PLoS One 6*(12), e26829.

Rue, H., A. Riebler, S. H. Sørbye, J. B. Illian, D. P. Simpson, and F. K. Lindgren (2017). Bayesian computing with inla: a review. *Annual Review of Statistics and Its Application 4*, 395–421.

Santos-Fernandez, E., E. E. Peterson, J. Vercelloni, E. Rushworth, and K. Mengersen (2021). Correcting misclassification errors in crowdsourced ecological data: A bayesian perspective. *Journal of the Royal Statistical Society: Series C (Applied Statistics) 70*(1), 147–173.

Tanner, J. E. (2017). Multi-decadal analysis reveals contrasting patterns of resilience and decline in coral assemblages. *Coral Reefs 36*(4), 1225–1233.

Tebbett, S. B., J. Morais, and D. R. Bellwood (2022). Spatial patchiness in change, recruitment, and recovery on coral reefs at lizard island following consecutive bleaching events. *Marine Environmental Research 173*, 105537.

Thilan, P. A. W. L., E. E. Peterson, P. Menendez, J. Caley, C. Drovandi, C. Mellin, and J. McGree (2019). Bayesian design methods for improving the effectiveness of monitoring coral reefs.

712 Ver Hoef, J. M., E. E. Peterson, M. B. Hooten, E. M. Hanks, and M.-J. Fortin
713 (2018). Spatial autoregressive models for statistical inference from ecological
714 data. *Ecological Monographs 88*(1), 36–59.

715 Vercelloni, J., B. Liquet, E. V. Kennedy, M. González-Rivero, M. J. Caley, E. E.
716 Peterson, M. Puotinen, O. Hoegh-Guldberg, and K. Mengersen (2020). Fore-
717 casting intensifying disturbance effects on coral reefs. *Global Change Biol-*
718 *ogy 26*(5), 2785–2797.

719 Vercelloni, J., K. Mengersen, F. Ruggeri, and M. J. Caley (2017). Improved coral
720 population estimation reveals trends at multiple scales on australia's great bar-
721 rier reef. *Ecosystems 20*(7), 1337–1350.

722 Warne, D. J., K. A. Crossman, W. Jin, K. Mengersen, K. Osborne, M. J. Simp-
723 son, A. A. Thompson, P. Wu, and J.-C. Ortiz (2022). Identification of two-
724 phase recovery for interpretation of coral reef monitoring data. *Journal of*
725 *Applied Ecology 59*(1), 153–164.

726 Wikle, C. K. and A. Zammit-Mangion (2022). Statistical deep learning for spa-
727 tial and spatio-temporal data. *arXiv preprint arXiv:2206.02218*.

728 Wolff, N. H., P. J. Mumby, M. Devlin, and K. R. Anthony (2018). Vulnerability
729 of the great barrier reef to climate change and local pressures. *Global change*
730 *biology 24*(5), 1978–1991.

731 Zurell, D., C. König, A.-K. Malchow, S. Kapitza, G. Bocedi, J. Travis, and

732 G. Fandos (2022). Spatially explicit models for decision-making in animal
733 conservation and restoration. *Ecography 2022*(4).

Figure captions

Figure 1: Locations of the data and spatial predictions. a) Dots show the locations of surveyed 100m sub-sites across Heron Island Reef and geomorphic zones b) Predictive locations used in the spatio-temporal model. The boxed area indicates the area used to interpret the indicators of coral recovery. Data available from the Pangea Digital Repository: `https://doi.pangaea.de/10.1594/PANGAEA.907025`.

Figure 2: Long-term trajectories of cover estimated by the model at the habitat scale for a) branching, b) plate, and c) massive corals. The dots and error bars denote the observed values and associated 95% confidence intervals. The line and shaded areas are the model estimates showing the mean and 95% credible intervals estimated from the model posterior distributions. Note that the y-axis is on a different scale for the massive corals in panel c.

Figure 3: Spatial and temporal changes in branching corals. a) Predicted coral cover estimated at unobserved locations between 2002-2018, b) Temporal changes of the probability of recovery at the habitat scale. The dotted line shows the threshold of successful recovery and c) Estimated growth rate at the habitat scale across years.

Figure 4: Spatial and temporal changes in plate corals. a) Predicted coral cover

estimated at unobserved locations between 2002-2018, b) Temporal changes of the probability of recovery at the habitat scale. The dotted line shows the threshold of successful recovery and c) Estimated growth rate at the habitat scale across years.

Figure 5: Indicators of recovery for branching corals. a) Predictive locations on the reef slope on which branching corals recovered or not using the 75% chance of recovery across 2008-2018 as threshold, b) Associated levels of relative decline estimated from the overall distribution within the reef slope of the small area, c) Associated levels of baseline cover estimated from the overall distribution within reef slope of the small area and d) Temporal changes of the branching absolute growth rate in y^{-2} between 2010 and 2018 for the south reef slope. Line colours denote the presence and absence of recovery at the predictive locations, and the solid black line shows the growth rate threshold of recovery estimated by the logistic model.

Figure 6: Indicators of recovery for plate corals. a) Predictive locations on the reef slope on which branching corals recovered or not using the 75% chance of recovery across 2008-2018 as threshold, b) associated levels of relative decline estimated from the overall distribution within the reef slope of the small area, c) Associated levels of baseline cover estimated from the overall distribution within reef slope of the small area and, d) Temporal changes of the branching absolute growth rate in y^{-2} between 2010 and 2018 for the south reef slope. Line colours

denote the presence and absence of recovery at the predictive locations, and the solid black line shows the growth rate threshold of recovery estimated by the logistic model.

Figures

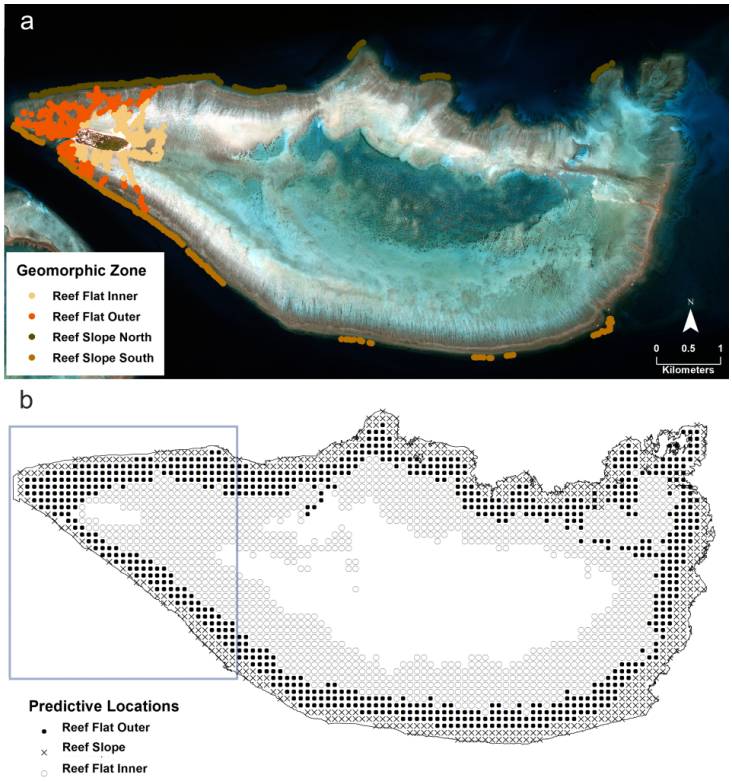

Figure 1

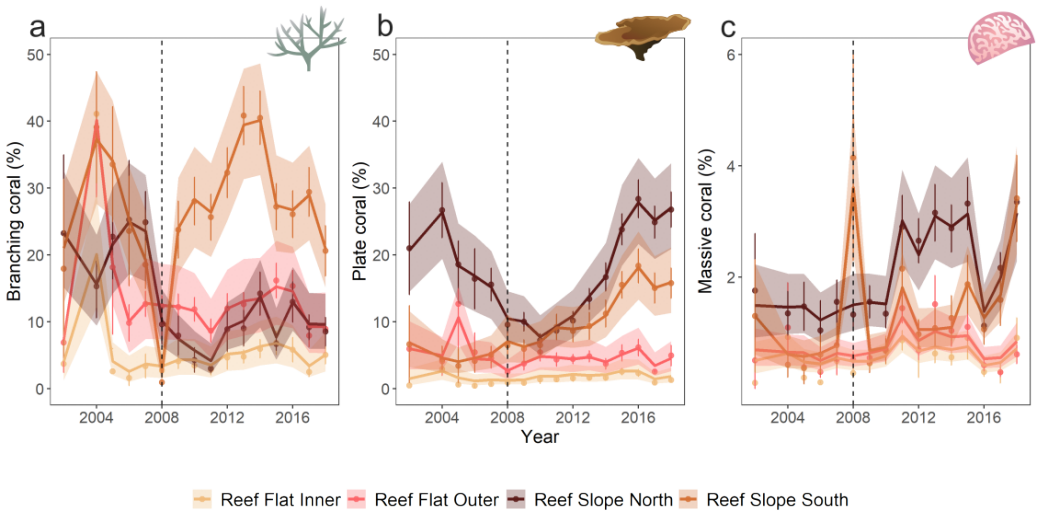
a
b
c
Branching coral (%)
Plate coral (%)
Massive coral (%)
Year
2004
2008
2012
2016
Reef Flat Inner
Reef Flat Outer
Reef Slope North
Reef Slope South

Figure 2

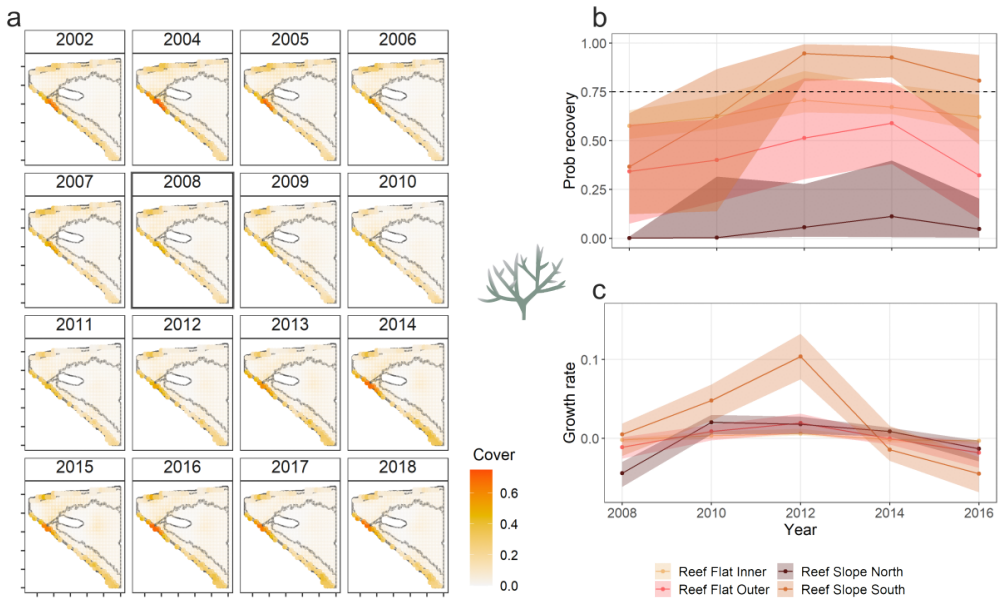
a
2002
2004
2005
2006
2007
2008
2009
2010
2011
2012
2013
2014
2015
2016
2017
2018
Cover
0.6
0.4
0.2
0.0
b
Prob recovery
1.00
0.75
0.50
0.25
0.00
c
Growth rate
0.1
0.0
2008
2010
2012
2014
2016
Year
Reef Flat Inner
Reef Flat Outer
Reef Slope North
Reef Slope South

Figure 3

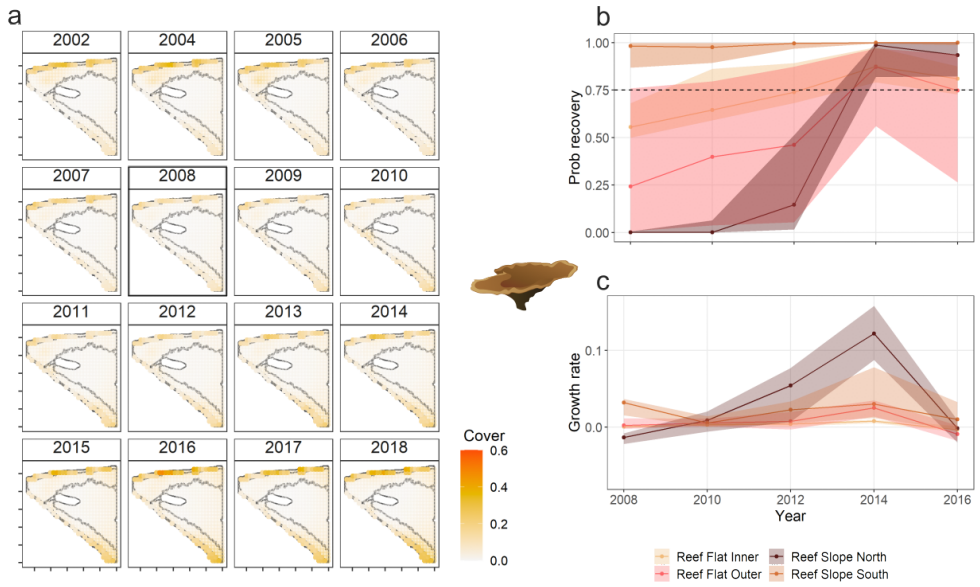
a
2002
2004
2005
2006
2007
2008
2009
2010
2011
2012
2013
2014
2015
2016
2017
2018
Cover
0.6
0.4
0.2
0.0
b
Prob recovery
1.00
0.75
0.50
0.25
0.00
c
Growth rate
0.1
0.0
2008
2010
2012
2014
2016
Year
Reef Flat Inner
Reef Flat Outer
Reef Slope North
Reef Slope South

Figure 4

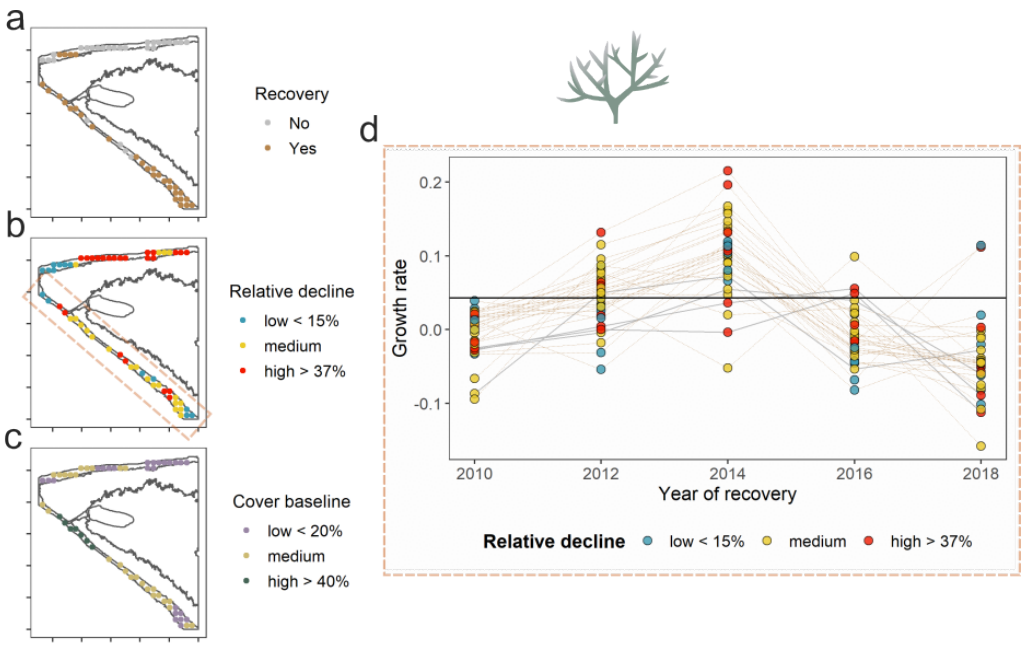
a
b
c
d
Recovery
No
Yes
Relative decline
low < 15%
medium
high > 37%
Cover baseline
low < 20%
medium
high > 40%
Growth rate
0.2
0.1
0.0
-0.1
2010
2012
2014
2016
2018
Year of recovery
Relative decline
low < 15%
medium
high > 37%

Figure 5

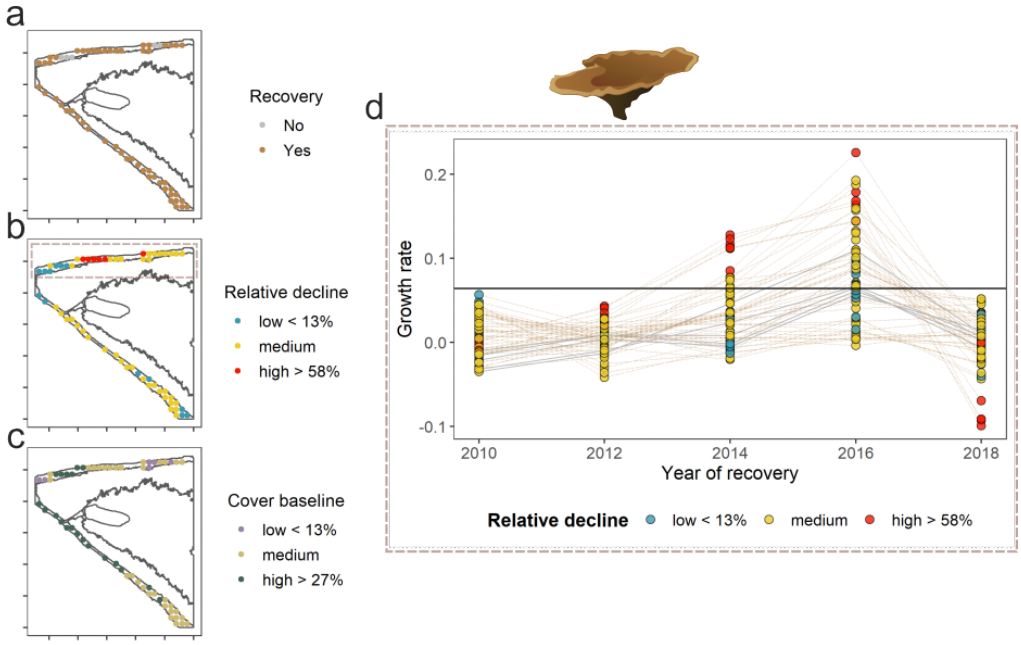
a
b
c
d
Recovery
No
Yes
Relative decline
low < 13%
medium
high > 58%
Cover baseline
low < 13%
medium
high > 27%
Growth rate
0.2
0.1
0.0
-0.1
2010
2012
2014
2016
2018
Year of recovery
Relative decline
low < 13%
medium
high > 58%

Figure 6